Effects of Strain and Damage on Strain-Sensing Ability of Carbon Fiber Cement

Sihai Wen[1] and D. D. L. Chung[2]

Abstract: The strain-sensing ability of carbon fiber cement, as based on piezoresistivity, remains in the presence of damage, although the gauge factor (fractional change in resistance per unit strain) is affected by strain and damage. The longitudinal gauge factor is diminished by compressive strain by up to 70% and by damage by up to 25%. The magnitude of the transverse gauge factor is diminished by strain by up to 60% and by up to 25% by minor damage not accompanied by irreversible strain, but it is increased by up to 120% by major damage accompanied by irreversible strain. The gauge factor, whether longitudinal or transverse, is reduced in magnitude as the specimen size increases (by 13 to 51 mm).

DOI: 10.1061/(ASCE)0899-1561(2006)18:3(355)

CE Database subject headings: Strain; Damage; Sensors; Fiber reinforced materials; Cement.

Introduction

Cement reinforced with short carbon fiber has been shown to be effective for sensing its own strain, due to the reversible effect of strain on the volume electrical resistivity (Chen and Chung 1993, 1996; Chung 2002a,b; Fu and Chung 1997; Fu et al. 1998; Mao et al. 1996; Reza et al. 2003; Sun et al., 1998; Wen and Chung 2000, 2001a,b, 2003, 2005; Yao et al. 2003). Upon compression the resistivity decreases reversibly. Upon tension, the resistivity increases reversibly. However, the effect is different when the curing age is only 7 days (Chen and Chung 1996; Reza et al. 2003). This effect, known as piezoresistivity, is a self-sensing ability that is valuable for structural vibration control, traffic monitoring, weighing, border security, room occupancy monitoring, and building facility management.

As a real concrete structure may be strained at different amplitudes and may also be damaged or cracked at certain locations (such as the tension side of a beam under flexure), the effects of strain and damage on the strain-sensing ability need to be investigated. Carbon fiber cement is capable of damage sensing, as the electrical resistivity increases irreversibly upon damage (Bontea et al. 2000; Chung 2003; Fu and Chung 1996, 1997; Reza et al. 2003; Wen and Chung 2006; Yao et al. 2003). In spite of this irreversible resistivity increase, the piezoresistivity behavior is maintained, at least qualitatively.

It has been shown during fatigue testing that the piezoresistive behavior is maintained up to failure, whether under cyclic tension or cyclic compression (Fu and Chung 1996). However, quantitative strain sensing requires an effect that is quantitative, not just qualitative. The fractional change in resistance per unit strain is known as the gauge factor, which quantitatively describes the piezoresistive behavior. The possible effects of strain and damage on the gauge factor have not been previously investigated. If the gauge factor is indeed affected by strain or damage, the gauge factor corresponding to a particular state of strain or damage, rather than that of the unstrained or undamaged state, should be used for the purpose of quantitative strain sensing in the strained or damaged state.

This paper is aimed at quantitative evaluation of the effects of strain and damage on the strain-sensing behavior of carbon fiber cement. The evaluation involves measurement of the longitudinal and transverse gauge factors under compression at different strain amplitudes. The longitudinal gauge factor is the fractional change in longitudinal resistance per unit of longitudinal strain, and the transverse gauge factor is the fractional change in transverse resistance per unit of transverse strain.

Experimental Methods

The carbon fibers were isotropic pitch based and unsized, as obtained from Ashland Petroleum Co. (Ashland, Ky.). The fiber diameter was 15 μm and the nominal fiber length was 5 mm. Fibers in the amount of 0.50% by mass of cement (corresponding to 0.48% of sample volume) were used. The percolation threshold is between 0.5 and 1.0% of sample volume (Fu and Chung 1997). Prior to using the fibers in cement, they were dried at 110°C in air for 1 h and then surface treated with ozone by exposure to O_3 gas (0.6% of sample volume, in O_2) at 160°C for 10 min. The ozone treatment was for improving the wettability of fibers by water (Fu et al. 1998).

The cement used was Portland cement (Type I) from Lafarge Corp. (Southfield, Mich.). The silica fume (Elkem Materials Inc., Pittsburgh, Pa., microsilica, EMS 965) was used in the amount of 15% by mass of cement. The methylcellulose, used in the amount of 0.4% by mass of cement, was Methocel A15-LV (Dow Chemi-

[1]Postdoctoral Associate, Dept. of Mechanical and Aerospace Engineering, Univ. at Buffalo, State Univ. of New York, Buffalo, NY 14260. E-mail: sihaiwen@buffalo.edu

[2]National Grid Endowed Chair Professor of Materials Research, Univ. at Buffalo, State Univ. of New York, Buffalo, NY 14260 (corresponding author). E-mail: ddlchung@buffalo.edu

Note. Associate Editor: Kolluru V. Subramaniam. Discussion open until November 1, 2006. Separate discussions must be submitted for individual papers. To extend the closing date by one month, a written request must be filed with the ASCE Managing Editor. The manuscript for this paper was submitted for review and possible publication on July 12, 2004; approved on November 30, 2004. This paper is part of the ***Journal of Materials in Civil Engineering***, Vol. 18, No. 3, June 1, 2006. ©ASCE, ISSN 0899-1561/2006/3-355–360/$25.00.

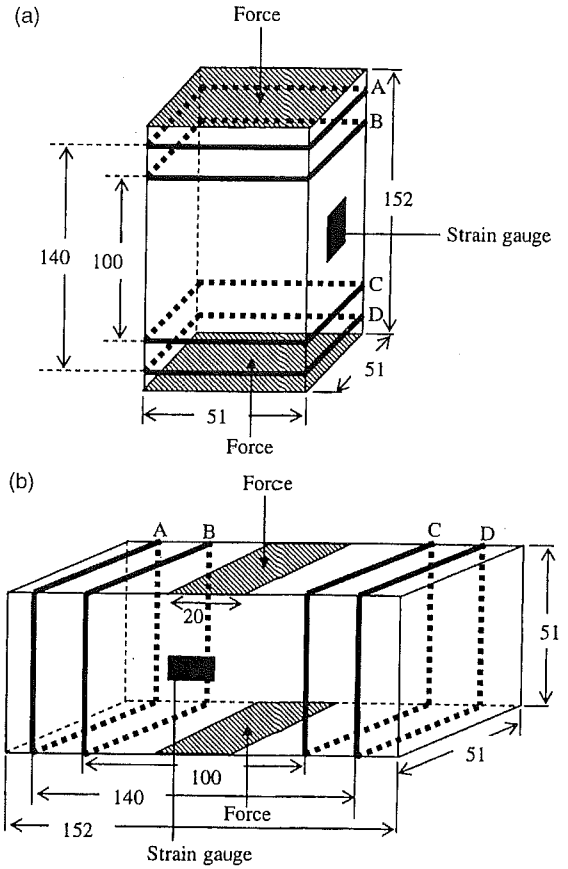

Fig. 1. Rectangular specimen configuration for separate measurements of (a) longitudinal resistance and (b) transverse resistance (all dimensions in mm)

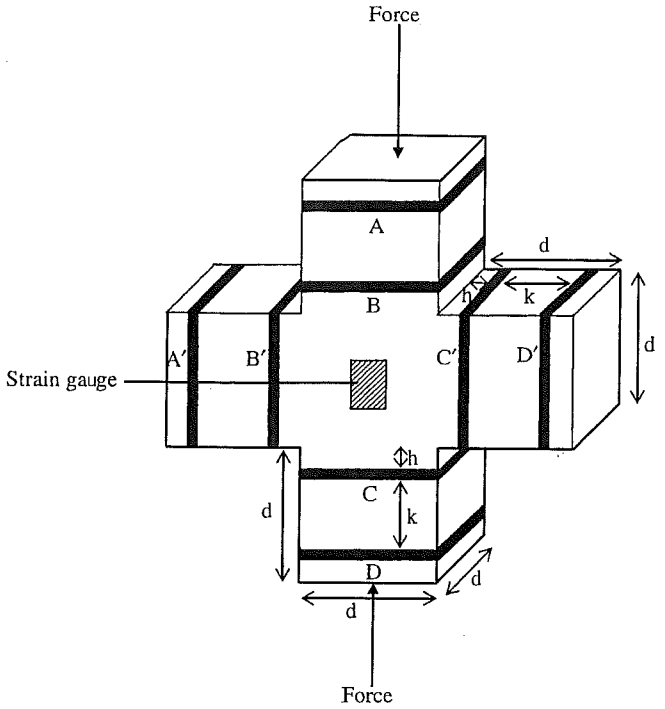

Fig. 2. Cross-shaped specimen configuration for simultaneous measurement of longitudinal and transverse resistances. d=13, 25, or 51 mm, d=13 mm, h=2 and k=8 mm, and for d=25 or 51 mm, h=5 and k=10 mm

cal Corp., Midland, Mich.). The defoamer (Colloids Inc., Marietta, Ga., 1010) used whenever methylcellulose was used was in the amount of 0.13% of sample volume.

A rotary mixer with a flat beater was used for mixing, and methylcellulose was dissolved in water and then the defoamer and fibers were added and stirred by hand for about 2 min. Then the methylcellulose mixture, cement, water, and silica fume were mixed for 5 min. After pouring the mix into oiled molds, an external electric vibrator was used to facilitate compaction and decrease the amount of air bubbles. The specimens were demolded after 1 day and then allowed to cure at room temperature in air (relative humidity=100%) for 28 days. The water/cement ratio was 0.35.

Specimens of the rectangular shape depicted in Fig. 1 were used for separate measurements of longitudinal and transverse resistances. In both Figs. 1(a and b), the specimen size was $6\times2\times2$ in. ($152\times51\times51$ mm), and the four electrical contacts (in the form of silver paint in conjunction with copper wire) were placed perimetrically around the specimen in four parallel planes perpendicular to the length of the specimen. The four contacts, labeled A, B, C, and D, were such that A and D (140 mm apart) were for passing current and B and C (100 mm apart) were for voltage measurement. Compressive force was applied on the entire 51×51 mm cross section of the specimen [shaded area in Fig. 1(a)] for the purpose of measuring the longitudinal resistance under compression in the same direction. In contrast, compressive force was applied only on the 51×20 mm shaded area in Fig. 1(b) for the purpose of measuring the transverse resistance under compression in the longitudinal direction. Three specimens were tested in the configuration of Fig. 1(a), and three other specimens were tested in the configuration of Fig. 1(b).

Specimens of the cross shape depicted in Fig. 2 were used for simultaneous measurement of longitudinal and transverse resistivities under uniaxial compression in the longitudinal direction and for studying the specimen size effect. They were prepared by using molds of the same shape, such that the vertical direction during curing was the direction perpendicular to the page in Fig. 2. For the same cross shape, three specimen sizes were obtained by using three mold sizes. The three sizes correspond to d (specimen dimension defined in Fig. 2) being 0.5, 1.0, and 2.0 in. (13, 25, and 51 mm); six specimens of each size were tested.

During repeated compression, DC electrical resistance measurement in the longitudinal direction was made by using the electrical contacts A, B, C, and D, as shown in Fig. 2. Each contact was in the form of silver paint in conjunction with copper wire, which was wound perimetrically. In accordance with the four-probe method of resistance measurement, contacts A and D were for passing current while contacts B and C were for measuring the voltage. As contacts B and C were close to the central cubic portion (2 to 5 mm from the edge of the central cubic portion) of the specimen (i.e., the portion experiencing the stress), the measured resistance was essentially the longitudinal resistance of the central cubic portion. Similarly, electrical resistance in the transverse direction was measured by using electrical contacts A', B', C', and D', as shown in Fig. 2. Because the strains involved were small, the fractional change in resistance was essentially equal to the fractional change in resistivity.

Uniaxial compressive stress at increasing amplitudes was applied in the direction shown in Figs. 1 and 2. The stress was provided by a hydraulic mechanical testing system (MTS Systems Corp., Model 810). In Fig. 2, the loading time in a cycle was

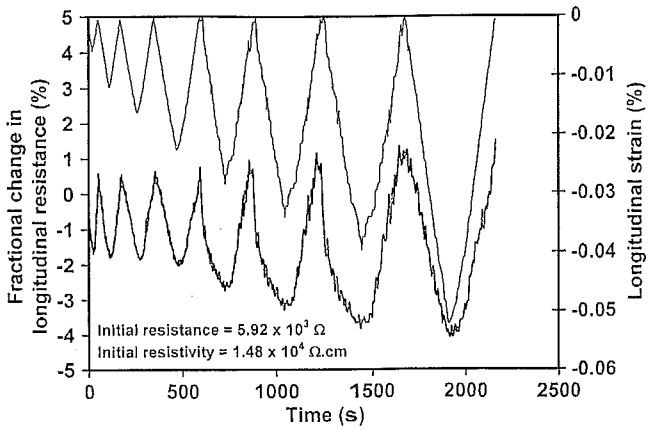

Fig. 3. Variation of fractional change in longitudinal resistance (thick curve) and longitudinal strain (thin curve) with time during uniaxial compression at progressively increasing stress amplitudes in elastic regime

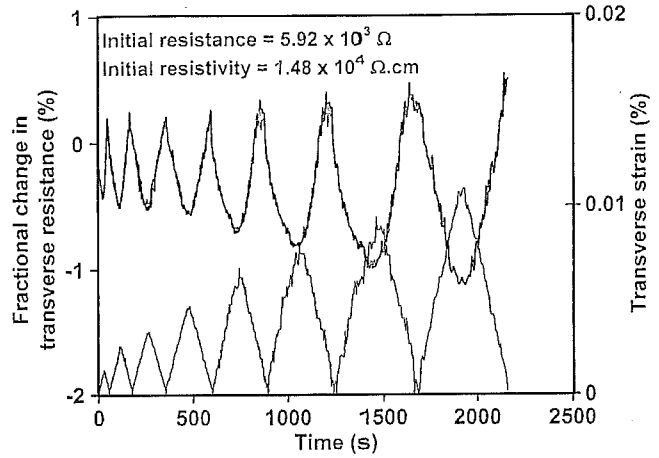

Fig. 4. Variation of fractional change in longitudinal resistance (thick curve) and transverse strain (thin curve) with time during uniaxial compression at progressively increasing stress amplitudes in elastic regime

fixed, while in Fig. 1 the loading rate was fixed at 0.014 MPa/s. A strain gauge was applied to the center of the specimen in Fig. 2, one on each of two opposite surfaces. One strain gauge was for measuring the longitudinal strain and the other for measuring the transverse strain. A strain gauge was applied at the center of the specimen of Figs. 1(a and b) for measuring the longitudinal and transverse strains, respectively.

The configurations in Figs. 1 and 2 also allow measurement of the resistivity at no load. The dependence of the resistivity on fiber volume fraction and specimen size was thus studied in this work using the configuration in Fig. 2. At no load, the resistivity is the same in the longitudinal and transverse directions.

Results and Discussion

The resistivity is $(1.24\pm0.07)\times10^4$, $(1.33\pm0.10)\times10^4$, and $(1.49\pm0.08)\times10^4\ \Omega$ cm for small (d=13 mm, Fig. 2), medium (d=25 mm, Fig. 2), and large (d=51 mm, Fig. 2) specimens, respectively. The decrease in resistivity as the specimen size decreases is attributed to the increase in the degree of fiber-preferred orientation in the plane of Fig. 2.

Effect of Strain

Figs. 3 and 4, obtained using the configurations of Fig. 1(a and b), respectively, show that both the longitudinal and transverse resistances decrease upon compression due to piezoresistivity, as previously reported (Fu et al. 1998). This is due to the Poisson effect, where the transverse strain is positive while the longitudinal strain is negative. All the strain amplitudes in Figs. 3 and 4 were in the elastic regime. The gauge factor was calculated for each strain amplitude (i.e., for each cycle) by considering the reversible change in resistance for the particular cycle.

As shown in Table 1, the magnitude of the gauge factor decreases monotonically with increasing strain amplitude for both longitudinal and transverse cases. This trend may be related to the piezoresistivity being due to the fiber push-in upon compression (Chung 1995) and to the initial stage of push-in having more influence on the fiber-matrix contact resistivity than the later stage of push-in. Although the strain amplitude is much smaller in magnitude for the transverse case than the longitudinal case, the gauge factor is comparable in magnitude for the two cases (Table 1).

Effect of Damage

Fig. 5 (longitudinal case) and Fig. 6 (transverse case) were simultaneously obtained for the same specimen, using the configuration of Fig. 2. The strain amplitudes in Figs. 5 and 6 are much higher than those in Figs. 3 and 4. In particular, the strain amplitudes in Figs. 5 and 6 include those beyond the elastic limit. Both longitudinal and transverse resistivities decrease upon uniaxial compression, as in Figs. 3 and 4, but the strains as well as the resistivities show partial irreversibility after the third cycle, although the resistivities show slight partial irreversibility even after the first cycle, as shown clearly in Table 2. The irreversible resistivity change is an increase in all cases. The higher the stress amplitude, the more the irreversible change in resistivity and the irreversible strain.

The small irreversible resistivity changes after the first and second cycles (Table 2) indicate minor damage in the elastic regime (irreversible strain absent). The large irreversible resistivity changes after the third, fourth, and fifth cycles indicate major damage in the plastic deformation regime (irreversible strain present). The trends are the same for the longitudinal and transverse resistivities, though the magnitude of the transverse irreversible strain is smaller than that of the longitudinal irreversible strain, and the fractional irreversible resistivity change is accordingly lower in the transverse than in the longitudinal direction.

As shown in Table 2, the greater the cycle number, the greater were the irreversible strain and the irreversible resistivity change. The gauge factor was obtained by dividing the fractional change in resistance for the cycle (change relative to the resistance value at the beginning of the cycle) by the strain amplitude for the cycle.

As shown in Table 3, the longitudinal gauge factor decreases slightly with increasing strain amplitude, whereas the magnitude of the transverse gauge factor increases with strain amplitude at Cycle 3 and beyond. These trends apply to all three specimen sizes. As shown in Table 1, damage starts to become significant at Cycle 3. The occurrence of damage is supported by a decrease of 10% in both the compressive strength and the compressive modu-

Table 1. Gauge Factor for Each Cycle in Fig. 3 (Longitudinal Case) and Fig. 4 (Transverse Case)

Case	Cycle 1	Cycle 2	Cycle 3	Cycle 4	Cycle 5	Cycle 6	Cycle 7	Cycle 8
Longitudinal								
Strain amplitude (10^{-4})	−0.57±0.06	−1.17±0.18	−1.61±0.23	−2.24±0.28	−2.83±0.36	−3.40±0.44	−3.97±0.51	−5.18±0.66
Gauge factor	332±56	240±30	150±19	136±17	135±15	143±20	138±18	112±13
Transverse								
Strain amplitude (10^{-4})	0.13±0.02	0.26±0.03	0.34±0.04	0.47±0.06	0.67±0.08	0.81±0.11	0.94±0.12	1.09±0.15
Gauge factor	−360±47	−307±40	−261±31	−180±25	−168±23	−154±19	−141±16	−133±18

Note: Strain amplitude (elastic regime) increases with cycle number.

lus, as shown after Cycle 3 by separate compressive testing using cubic specimens of size 2×2×2 in. (51×51×51 mm). Thus damage causes the transverse gauge factor to increase in magnitude, whereas it causes the longitudinal gauge factor to decrease slightly. Damage enhances the transverse piezoresistive effect because the transverse direction experiences tension, which tends to enhance microcracking, thereby intensifying the fiber pull-out associated with piezoresistivity. Damage does not affect the Poisson ratio, which remains at 0.21 in all cycles. Damage diminishes the longitudinal piezoresistive effect because it interferes with the fiber push-in that accompanies the piezoresistive effect under compression.

In the regime of minor damage (Cycles 1 and 2), the transverse gauge factor diminishes slightly in magnitude upon damage (Table 2). This decrease is probably because minor damage interferes with the fiber pull-out that accompanies the piezoresistive effect under tension. The crack opening that accompanies major damage does not occur sufficiently during minor damage to help the piezoresistivity.

For all three specimen sizes, the longitudinal gauge factor is decreased by up to 25% upon damage accompanied by irreversible strain, and the magnitude of the transverse gauge factor is increased by up to 120% upon damage accompanied by irreversible strain. Minor damage not accompanied by irreversible strain diminishes the magnitude of both the transverse and longitudinal gauge factors by up to 25%.

The values of the gauge factor magnitude are considerably lower in Table 3 than Table 1. This is due to the high strain amplitudes for Table 3 (strain amplitudes shown in Table 2) compared to those for Table 1 and to the trend (Table 1) of the gauge factor magnitude to decrease with increasing magnitude of the strain amplitude.

Effect of Specimen Size

The general behavior is the same for the three specimen sizes, as shown in Table 2. However, for each stress amplitude in the regime of major damage (i.e., cycles 3 to 5), the small size is associated with a greater irreversible strain magnitude and a higher irreversible resistivity fractional change than the medium and large sizes, whether the direction is longitudinal or transverse. This is attributed to the higher chance of close proximity of some microcracks to the specimen surface in the case of the small specimen size and the consequent greater ease for microcrack propagation.

In the regime of minor damage (i.e., Cycles 1 and 2), the effect of specimen size on the fractional irreversible change in resistivity is small, though there is a tendency for this fractional change (whether longitudinal or transverse) to increase with increasing specimen size. This tendency is attributed to the increase in the degree of 2D (in the plane including both transverse and longitudinal directions) fiber alignment as the specimen size decreases, as indicated by the decrease in resistivity as the specimen size decreases (mentioned in the first paragraph of the results and discussion section). More fiber alignment will result in less propensity to damage, even though the damage is minor, while less damage in turn results in a smaller fractional irreversible resistivity change.

The irreversible strain and fractional irreversible resistivity

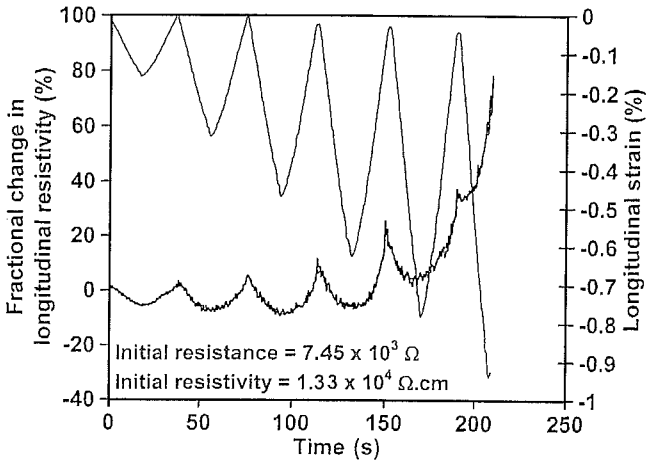

Fig. 5. Variation of fractional change in longitudinal resistivity (thick curve) and longitudinal strain (thin curve) with time during uniaxial compression at progressively increasing stress amplitudes (specimen size is medium)

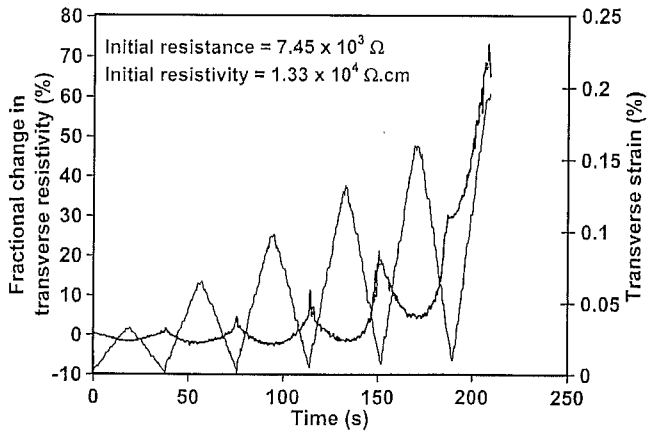

Fig. 6. Variation of fractional change in transverse resistivity (thick curve) and transverse strain (thin curve) with time during uniaxial compression at progressively increasing stress amplitudes (specimen size is medium)

Table 2. Irreversible Strain and Resistivity Change after Various Numbers of Cycles of Compressive Loading at Progressively Increasing Stress Amplitudes up to Failure

Cycle number	Specimen size	Strain amplitude (%)		Irreversible strain (10^{-4})[a]		Irreversible resistivity change (%)[a]	
		Longitudinal	Transverse	Longitudinal	Transverse	Longitudinal	Transverse
1	Small	−0.146±0.018	0.029±0.003	0	0	2.40±0.12	1.41±0.08
	Medium	−0.152±0.019	0.033±0.004	0	0	2.59±0.15	1.56±0.07
	Large	−0.148±0.020	0.032±0.004	0	0	3.16±0.23	1.64±0.06
2	Small	−0.300±0.036	0.057±0.006	0	0	4.80±0.34	3.50±0.27
	Medium	−0.308±0.040	0.065±0.071	0	0	5.40±0.31	4.50±0.41
	Large	−0.299±0.033	0.068±0.008	0	0	6.50±0.28	5.45±0.33
3	Small	−0.449±0.051	0.090±0.013	−3.7±0.2	0.85±0.05	16.9±1.5	13.1±1.2
	Medium	−0.469±0.057	0.098±0.012	−2.3±0.2	0.50±0.03	11.5±1.1	11.2±0.9
	Large	−0.443±0.055	0.102±0.015	−2.0±0.1	0.50±0.02	14.3±1.2	10.4±0.7
4	Small	−0.599±0.070	0.120±0.016	−4.8±0.3	1.00±0.07	30.0±1.9	26.2±1.7
	Medium	−0.621±0.070	0.131±0.013	−2.9±0.1	0.70±0.04	25.0±1.3	21.3±1.2
	Large	−0.596±0.076	0.132±0.020	−2.7±0.2	0.60±0.03	24.4±0.9	20.5±1.5
5	Small	−0.749±0.100	0.151±0.020	−5.7±0.6	1.3±0.1	46.5±3.8	32.0±2.5
	Medium	−0.782±0.082	0.159±0.019	−4.5±0.4	1.1±0.1	36.7±3.3	29.4±2.1
	Large	−0.738±0.090	0.169±0.022	−4.3±0.3	1.0±0.1	32.0±2.7	28.9±2.1

Note: Failure occurs in Cycle 6 in Figs. 5 and 6. Strain amplitude increases in magnitude with cycle number.

[a]Relative to value prior to loading.

change are quite close for the medium and large specimens for each cycle, whether the direction is longitudinal or transverse (Table 2). This means that for a specimen size larger than medium (d=25 mm, Fig. 2), the specimen size has little effect on the damage-sensing characteristics. For structures much larger than 25 mm in dimension, the results given in this paper for medium and large sizes may apply. However, in relation to the use of carbon fiber cement as a coating for strain sensing (Wen and Chung 2001a), the results given in this paper for the small size may apply.

Table 3 shows the gauge factor for each cycle of Figs. 5 and 6 in both the longitudinal and transverse directions. The magnitude of both of these gauge factors decreases with increasing specimen size. This is because of the decrease in the degree of fiber-preferred orientation in the plane of Fig. 2.

The longitudinal gauge factor is diminished by 30% upon increasing the specimen size (d in Fig. 2) from 13 to 51 mm. Most of the gauge factor decrease occurred as the specimen size was increased from 13 to 25 mm. The magnitude of the transverse gauge factor is decreased by up to 50% upon increase of the specimen size from 13 to 51 mm.

Practical Strain Sensing

The observed effect of strain amplitude on the gauge factor means that quantitative strain sensing using carbon fiber cement requires selection of a gauge factor value suitable for the range of strain to be sensed. The gauge factor is highest for the smallest strain amplitude (−0.005%), so carbon fiber cement is most effective for the sensing of small strains. In addition, strain sensing can be performed by using a gauge factor programmed to vary with the irreversible resistivity fractional change. The large specimen size is most relevant to real structures. The data in Tables 2 and 3 in combination suggest the following example of a practical procedure for strain sensing. For the case of the large specimen size, when the irreversible longitudinal resistivity reaches 10 to 20%, the longitudinal gauge factor would be changed from 32 to 28; when the irreversible transverse resistivity reaches 7 to 13%, the transverse gauge factor would be changed from −35 to −67.

Conclusion

Both strain and damage (whether or not the damage is accompanied by irreversible strain) diminish the longitudinal piezoresis-

Table 3. Gauge Factor in Longitudinal and Transverse Directions for Three Specimen Sizes

Cycle number	Gauge factor					
	Longitudinal			Transverse		
	Small	Medium	Large	Small	Medium	Large
1	48.3±3.3	36.1±2.7	34.5±2.8	−62.1±4.7	−51.7±4.1	−46.3±3.3
2	44.5±4.1	32.3±2.4	31.5±2.9	−54.9±4.2	−46.1±3.7	−34.7±3.2
3	43.0±3.9	29.1±3.1	28.4±3.1	−85.7±7.2	−69.7±7.4	−67.3±6.0
4	40.7±4.7	28.0±3.2	27.3±3.6	−134.2±12.8	−96.6±10.2	−72.2±8.1
5	38.4±4.8	27.5±2.9	26.7±3.2	−138.8±15.6	−100.4±11.0	−88.6±9.3

Note: Specimen sizes are small, medium, and large, based on results in Figs. 5 and 6.

tive effect in carbon fiber cement. The longitudinal gauge factor is decreased by up to 70% due to increasing longitudinal strain magnitude (from 0.005 to 0.05%) and is decreased by up to 25% due to damage. The corresponding transverse gauge factor magnitude is decreased by up to 60% due to strain. Minor damage not accompanied by irreversible strain diminishes the magnitude of the transverse gauge factor by up to 25%, but major damage accompanied by irreversible strain enhances the transverse piezoresistive effect, increasing the magnitude of the gauge factor by up to 120%. Strain sensing based on piezoresistivity is effective even in the presence of major damage. The gauge factor magnitude decreases with increasing specimen size (13 to 51 mm) due to the decrease in the degree of fiber-preferred orientation. The strain-sensing ability is best for small strains (such as –0.005%), no damage, and small specimen size (such as 13 mm), although the ability remains for all combinations of strain, damage, and specimen size.

Acknowledgment

This work was supported in part by the National Science Foundation.

References

Bontea, D.-M., Chung, D. D. L., and Lee, G. C. (2000). "Damage in carbon fiber reinforced concrete, monitored by electrical resistance measurement." *Cem. Concr. Res.*, 30(4), 651–659.

Chen, P.-W., and Chung, D. D. L. (1993). "Carbon fiber reinforced concrete as a smart material capable of nondestructive flaw detection." *Smart Mater. Struct.*, 2(1), 22–30.

Chen, P.-W., and Chung, D. D. L. (1996). "Concrete as a new strain/stress sensor." *Composites, Part B*, 27B, 11–23.

Chung, D. D. L. (1995). "Strain sensors based on the electrical resistance change accompanying the reversible pull-out of conducting short fibers in a less conducting matrix." *Smart Mater. Struct.*, 4(1), 59–61.

Chung, D. D. L. (2003). "Damage in cement-based materials, studied by electrical resistance measurement." *Mater. Sci. Eng., R.*, 42(1), 1–40.

Chung, D. D. L. (2002a). "Electrical conduction behavior of cement-matrix composites." *J. Mater. Eng. Perform.*, 11(2), 194–204.

Chung, D. D. L. (2002b). "Piezoresistive cement-based materials for strain sensing." *J. Intell. Mater. Syst. Struct.*, 13(9), 599–609.

Fu, X., and Chung, D. D. L. (1996). "Self-monitoring of fatigue damage in carbon fiber reinforced cement." *Cem. Concr. Res.*, 26(1), 15–20.

Fu, X., and Chung, D. D. L. (1997). "Effect of curing age on the self-monitoring behavior of carbon fiber reinforced mortar." *Cem. Concr. Res.*, 27(9), 1313–1318.

Fu, X., Lu, W., and Chung, D. D. L. (1998). "Ozone treatment of carbon fiber for reinforcing cement." *Carbon*, 36(9), 1337–1345.

Mao, Q., Zhao, B., Sheng, D., and Li, Z. (1996). "Resistance changement of compression sensible cement specimen under different stresses." *J Wuhan Univ. Tech.*, 11(3), 41–45.

Reza, F., Batson, G. B., Yamamuro, J. A., and Lee, J. S. (2003). "Resistance changes during compression of carbon fiber cement composites." *J. Mater. Civ. Eng.*, 15(5), 476–483.

Sun, M., Mao, Q., and Li, Z. (1998). "Size effect and loading rate dependence of the pressure-sensitivity of carbon fiber-reinforced concrete (CFRC)." *J. Wuhan Univ. Tech.*, 13(3), 58–61.

Wen, S., and Chung, D. D. L. (2000). "Uniaxial tension in carbon fiber reinforced cement, sensed by electrical resistivity measurement in longitudinal and transverse directions." *Cem. Concr. Res.*, 30(8), 1289–1294.

Wen, S., and Chung, D. D. L. (2001a). "Carbon fiber-reinforced cement as a strain-sensing coating." *Cem. Concr. Res.*, 31(4), 665–667.

Wen, S., and Chung, D. D. L. (2001b). "Uniaxial compression in carbon fiber reinforced cement, sensed by electrical resistivity measurement in longitudinal and transverse directions." *Cem. Concr. Res.*, 31(2), 297–301.

Wen, S., and Chung, D. D. L. (2003). "A comparative study of steel- and carbon-fibre cement as piezoresistive strain sensors." *Adv. Cem. Res.*, 15(3), 119–128.

Wen, S., and Chung, D. D. L. (2005). "Strain sensing characteristics of carbon fiber cement." *ACI Mater. J.*, 102(4), 244–248.

Wen, S., and Chung, D. D. L. (2006). "Damage sensing characteristics of carbon fiber cement." *Cem. Concr. Res.*, in press.

Yao, W., Chen, B., and Wu, K. (2003). "Smart behavior of carbon fiber-reinforced cement-based composite." *J. Mater. Sci. Tech.*, 19(3), 239–242.